






Article

Application of Real-Coded Genetic Algorithm–PID Cascade Speed Controller to Marine Gas Turbine Engine Based on Sensitivity Function Analysis

Yunhyung Lee ¹, Kitak Ryu ¹, Gunbaek So ², Jaesung Kwon ³ and Jongkap Ahn ^{4,*}

¹ Ocean Technology Training Team, Korea Institute of Maritime and Fisheries Technology, Busan 49111, Republic of Korea; domse54@daum.net (Y.L.); ryukitak@hanmail.net (K.R.)

² Department of Maritime Industry Convergence, Mokpo National Maritime University, Mokpo-si 58628, Republic of Korea; sgb@mmu.ac.kr

³ Department of Mechanical System Engineering, Gyeongsang National University, Tongyeong-si 53064, Republic of Korea; jkwon@gnu.ac.kr

⁴ Training Ship Operation Center, Gyeongsang National University, Tongyeong-si 53064, Republic of Korea

* Correspondence: jongkap.ahn@gnu.ac.kr; Tel.: +82-55-772-9042

Abstract: Gas turbine engines at sea, characterized by nonlinear behavior and parameter variations due to dynamic marine environments, pose challenges for precise speed control. The focus of this study was a COGAG system with four LM-2500 gas turbines. A third-order model with time delay was derived at three operating points using commissioning data to capture the engines' inherent characteristics. The cascade controller design employs a real-coded genetic algorithm–PID (R-PID) controller, optimizing PID parameters for each model. Simulations revealed that the R-PID controllers, optimized for robustness, show Nyquist path stability, maintaining the furthest distance from the critical point $(-1, j0)$. The smallest sensitivity function M_s (maximum sensitivity) values and minimal changes in M_s for uncertain plants confirm robustness against uncertainties. Comparing transient responses, the R-PID controller outperforms traditional methods like IMC and Sadeghi in total variation in control input, settling time, overshoot, and ITAE, despite a slightly slower rise time. However, controllers designed for specific operating points show decreased performance when applied beyond those points, with increased rise time, settling time, and overshoot, highlighting the need for operating-point-specific designs to ensure optimal performance. This research underscores the importance of tailored controller design for effective gas turbine engine management in marine applications.

Keywords: gas turbine engine; COGAG; genetic algorithm; maximum sensitivity

MSC: 93-10



Academic Editors: Adrian Olaru, Gabriel Frumusanu and Catalin Alexandru

Received: 26 December 2024

Revised: 15 January 2025

Accepted: 17 January 2025

Published: 19 January 2025

Citation: Lee, Y.; Ryu, K.; So, G.; Kwon, J.; Ahn, J. Application of Real-Coded Genetic Algorithm–PID Cascade Speed Controller to Marine Gas Turbine Engine Based on Sensitivity Function Analysis. *Mathematics* **2025**, *13*, 314. <https://doi.org/10.3390/math13020314>

Copyright: © 2025 by the authors. Licensee MDPI, Basel, Switzerland. This article is an open access article distributed under the terms and conditions of the Creative Commons Attribution (CC BY) license (<https://creativecommons.org/licenses/by/4.0/>).

1. Introduction

Gas turbine engines are mechanical devices that extract rotational mechanical energy by expanding high-temperature, high-pressure gas heated in a combustor, thus obtaining power. Gas turbines were first used at sea in the 1970s [1]. They are mainly applied for propulsion power and power supply in warships and marine plants [2,3]. Recently, marine gas turbines have started to be installed as auxiliary power units on merchant ships, such as large cruise ships like the Queen Mary II. They are expected to be increasingly adopted in other ship types due to their many advantages for shipowners [4], such as low weight, small volume, low noise, high availability, and reduced emissions of environmental

pollutants. They have low operating costs due to reduced lubricant consumption and maintenance work, which leads to reduced manpower requirements. Gas turbine engines also significantly contribute to reducing fuel costs, especially in high-speed ships. Due to their lightweight and small volume per unit output, they aid in the design of high-performance ships, and the system's reliability and availability of propulsion power are high [5,6].

The stable operation of gas turbine engines is critical in ensuring that the compressor rotors do not approach a crucial point where air pulsation and vibration occur during changes in rotational speed. It is essential to detect the maximum temperature and pressure according to the rotational speed and ensure a stable supply of fuel and air to the combustor to control the rotational speed of gas turbine engines precisely [7]. Therefore, it is very important to perform mathematical modeling and controller design that reflect gas turbine engines' complex internal structure and nonlinearity to achieve excellent speed control response in various marine environments.

In research on gas turbine engine modeling, Back et al. [8–10] conducted studies on engine performance by applying scaling techniques, employing the Constant Mass Flow (CMF) technique and the least squares method using experimental data.

Guda et al. [11] studied a microturbine power generation system driving a permanent magnet synchronous generator. Hannett et al. [12], Shin et al. [13], and Lee et al. [14] researched two-shaft turbine structures and fuel control valve characteristics.

In research related to controller design, Mohamed et al. [15] proposed a new strategy for implementing Model Predictive Control (MPC) in large gas turbine engine power plants. Lee et al. [16] proposed a speed controller for marine gas turbine engines using a nonlinear PID controller. Cha [17] developed and implemented an electronically controlled gas turbine engine control system in a simulator. Lee [18] designed an IMC-based PID speed controller using commissioning data from two LM-2500 propulsion gas turbine engines used in naval vessels.

Gas turbine engines have complex internal structures and model parameters that can vary depending on the characteristics of ships and marine environments, making the selection of controller parameters challenging. Additionally, simplified gas turbine engine models are commonly applied in modeling due to the lack of a standardized nonlinear model. Gas turbine engines are primarily used in naval vessels and are classified as military secrets. Moreover, their application in commercial ships is highly limited, making it challenging to accumulate or utilize relevant data. These factors pose significant difficulties in developing mathematical models and designing controllers for gas turbine engines.

In response, commissioning data from four LM-2500 gas turbine engines were utilized in the present study to model the engine by dividing it into an internal fuel metering unit (FMU) and a gas generator. A first-order model with time delay was applied to the gas generator, and a second-order linear model was used to represent the FMU. These were combined to derive a third-order model with a time delay for each of the three operating points. A real-coded genetic algorithm (RCGA)-PID controller (R-PID) was designed for speed control of the gas turbine engine. The controller design tunes the PID controller parameters using the RCGA to minimize the evaluation function based on the models obtained at each operating point. The effectiveness of the controller was verified using the sensitivity function.

The R-PID control system for speed control of marine gas turbine engines was quantitatively evaluated through simulation considering transient response characteristics, the influence of errors, and the total change in control input.

This study comprises six sections, including the introduction. Section 2 models a third-order gas turbine engine with a time delay. Section 3 introduces the real-coded

genetic algorithm as an optimization tool. Section 4 presents the design of the R-PID control system for speed control of the gas turbine engine. The RCGA was used to explore the parameters of the simplified FOPTD model and the R-PID controller’s parameters, as detailed in Section 5. The robustness of the controller was examined using the sensitivity function, and the tracking performance of the R-PID controller for nominal and uncertain plants at each operating point was confirmed through simulation. Section 6 summarizes the conclusions obtained in this study.

2. Modeling for Marine Gas Turbine Engine

The propulsion of the gas turbine engine involves rotating two propellers (port and starboard) using four gas turbine engines of exact specifications. The transfer function for the fuel quantity and rotational speed of the gas generator $G_E(s)$ can be obtained as follows.

$$G_E(s) = \frac{K_E}{1 + T_E s} e^{-L_E s}, \tag{1}$$

where K_E and T_E represent the gain and time constant of the gas generator, respectively. L_E is the time delay that occurs until the combustion gas reaches the rotor of the gas generator [19].

Table 1 summarizes the parameters for each operating point based on the commissioning data when four LM-2500 gas turbine engines are operated. The commissioning data are utilized at each operating point of LM-2500 gas turbine engines installed on ships with a COGAG (COmbined Gas turbine And Gas turbine) propulsion system. The pitch angle of the CPP (Controllable Pitch Propeller) is fixed for each speed, and it remains almost 100% at speeds above 7000 [r/min].

Table 1. Parameters of gas generator for LM-2500.

Model	$G_{E1}(s)$	$G_{E2}(s)$	$G_{E3}(s)$
Operating point	6500 [r/min]	7500 [r/min]	8500 [r/min]
Gain (K_E)	9.332	6.507	2.984
Time constant (T_E)	4.375	2.785	1.400
Time delay (L_E)	0.52	0.30	0.15

The Fuel Metering Actuator (FMA), which is a core component of the electronic FMU, is a device that changes the displacement of the spool to vary the fuel flow rate according to the input current. In Figure 1, the transfer function of the FMA $G_{FMA}(s)$ includes an integrator and is similar to a typical spool valve system [20]. K_{FMA} and T_{FMA} represent the gain and time constant of the FMA, respectively. K_u is a conversion constant that translates the control input of the FMU into the input current rate applied to the spool displacement of the FMA, and K_a is the proportional control gain of the FMA. K_b is a constant that converts the spool displacement of the FMA (in mm) into the ratio relative to the fuel flow rate q (in kg per hour). h_f is a conversion constant that translates the spool displacement of the FMA into the corresponding control input signal current value when feedback is provided through the LVDT (Linear Variable Differential Transformer). The overall transfer function of the FMU is summarized in (2), which is assumed to be independent of the operational point variations in the gas generator.

$$G_{FMU}(s) = \frac{Q(s)}{U(s)} = \frac{K_b K_{FMA} K_a K_u}{T_{FMA} s^2 + s + h_f K_{FMA} K_a}, \tag{2}$$

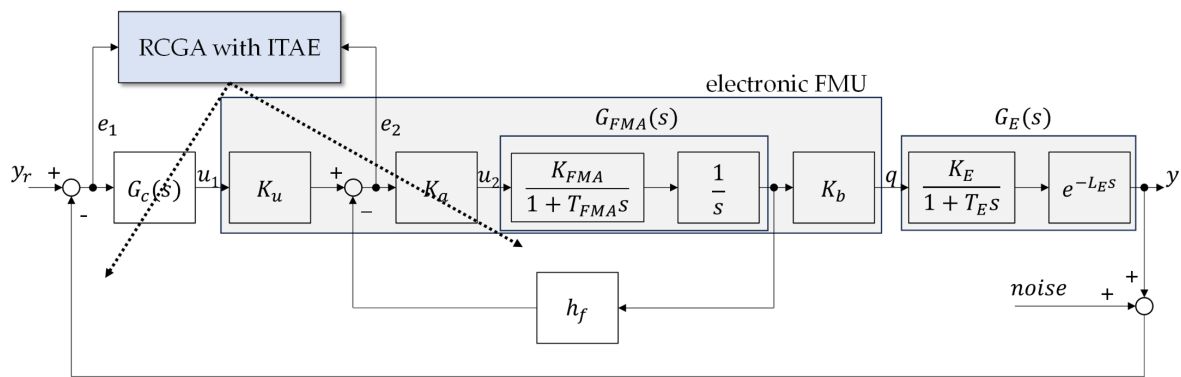


Figure 1. Block diagram of gas turbine engine speed control system with RCGA tuning.

Table 2 presents the parameters of the electronic FMU. The gain K_{FMA} and time constant T_{FMA} of the FMA are set according to Cha et al. [20]. The fuel flow constant K_b is differentiated according to the spool position and fuel quantity at each operating point.

Table 2. Parameters of fuel metering unit.

Parameters	Description	Value	Unit
K_u	FMA spool constant	0.8	-
K_a	Gain of amplifier	2	-
K_{FMA}	Gain of Fuel Metering Actuator	4	-
T_{FMA}	Time constant of Fuel Metering Actuator	0.1	[s]
h_f	Feedback gain of LVDT	0.8	[mA/mm]
K_b	Fuel flow rate	at 6500 [r/min]	155
	constant	at 7500 [r/min]	158
		at 8500 [r/min]	204

In a previous study [21], the amplifier gain K_a of the FMA was set to 2, considering its effect on the controller characteristics. However, the optimal gain value and PID controller parameters were explored in this study using the RCGA. The previously selected $K_a = 2$ was applied to the IMC controller, Sadeghi controller, LopezITAE controller, and Skogestad controller, which were considered for comparison purposes in this study with the simplified FOPTD model.

The entire gas turbine engine, which is the control target, can ultimately be summarized by integrating (1) and (2) into (3).

$$G_P(s) = \frac{K_E K_b K_{FMA} K_a K_u e^{-L_E s}}{T_E T_{FMA} s^3 + (T_E + T_{FMA}) s^2 + (1 + T_E h_f K_{FMA} K_a) s + h_f K_{FMA} K_a}, \quad (3)$$

The block diagram of the entire control system is briefly represented in Figure 1.

3. Real-Coded Genetic Algorithm as an Optimization Tool

As systems grow more extensive, with stronger interactions between variables and the inclusion of constraints, real-world optimization problems become increasingly complex. The search space for these problems often features multiple peaks, which can cause traditional gradient descent methods to converge to local solutions, and they cannot be applied if derivatives cannot be obtained. To address this, algorithms mimicking natural phenomena, such as genetic algorithms [22], simulated evolution [23], and evolutionary strategies [24], have been developed. These algorithms are successfully used in many fields, including system identification and control, machine learning, facility layout, neural networks, signal processing, and biotechnology, due to their advantage of not requiring

prior knowledge about the search space or auxiliary information beyond the objective function [25,26]. Genetic algorithms based on natural selection and genetics have traditionally operated on binary-coded chromosomes, and many genetic algorithms still employ binary coding. However, chromosome lengths can become excessive if users lack prior knowledge of the search space and choose a large definition domain or aim for high solution precision. Long chromosomes create large search spaces, increasing computational burdens and sometimes making searches infeasible [27]. The real-coded genetic algorithm (RCGA) offers several advantages over the binary-coded genetic algorithm (BCGA), particularly in optimization problems involving continuous variables. Unlike the BCGA, which requires binary encoding and decoding, the RCGA represents solutions directly as real numbers, eliminating unnecessary computational overhead. This direct representation allows for more precise search space exploration and enhances convergence efficiency. Additionally, the RCGA facilitates intuitive genetic operators, such as crossover and mutation, that operate seamlessly within a continuous domain. By reducing memory usage and improving computational efficiency, the RCGA is especially advantageous in high-dimensional optimization problems, offering superior accuracy and quality performance in solutions. The RCGA was utilized in this study to overcome these issues of the BCGA and effectively solve optimization problems. In the RCGA, chromosomes are represented as real-number vectors. The selection of parameters influences the search performance of the RCGA, so the optimal parameter domain is derived through an appropriate performance evaluation environment and method. The RCGA was used in this study to approximate a third-order time-delay system as a first-order time-delay system and to solve the controller optimization problem.

The initial population of the RCGA is randomly generated through a random number generator. Genetic operators used include reproduction similar to gradients [28], modified simple crossover [29], and dynamic mutation [30]. Additional strategies, such as the scaling window [30] and elite strategy [31], are applied. Figure 2 illustrates the basic structure of a genetic algorithm.

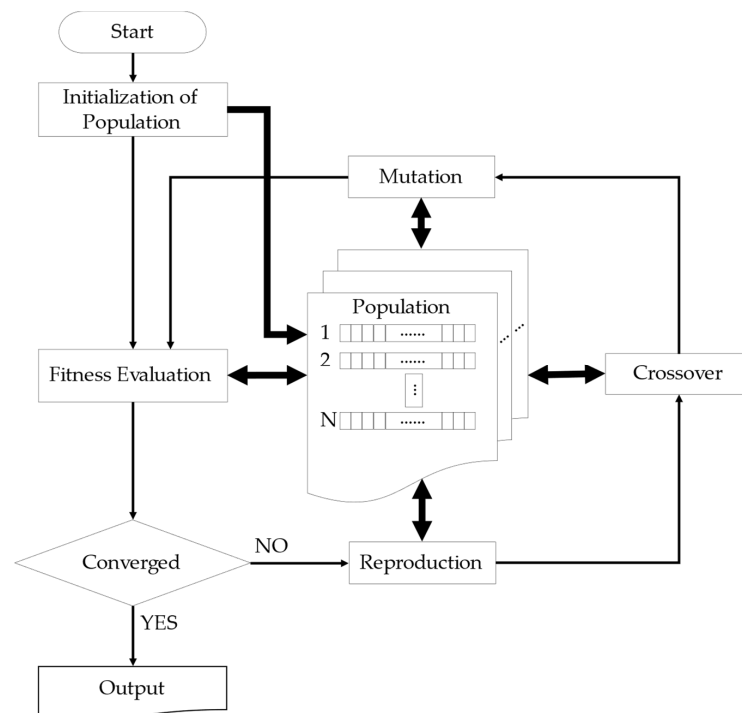


Figure 2. The basic structure of a GA.

4. Design of Speed Controller for Gas Turbine Engine

The following PID controller was designed to enable robust and stable speed control of the gas turbine engine.

$$u_1(t) = K_P \left(e_1(t) + \frac{1}{T_I} \int e_1(t)dt + T_D \frac{de_1(t)}{dt} \right), \tag{4a}$$

$$u_2(t) = K_a e_2(t), \tag{4b}$$

R-PID controllers for each operating point were designed using the third-order engine model from (3). The tuning method using the RCGA for selecting the optimal controller gains is shown in Figures 1 and 2. Each gene of the real-number chromosome is mapped one-to-one with the PID controller parameters K_P , T_I , T_D , and K_a in (4). Each gene is optimally tuned from the perspective of minimizing the objective function. The controllers tuned at the three operating points considered in this study, 6500 [r/min], 7500 [r/min], and 8500 [r/min], are defined as R-PID_i (i = 1, 2, 3). The RCGA searches the parameters of the R-PID controller within the given range to minimize the objective function in (5).

$$J = \int_0^{t_f} t \times (|e_1(t)| + 1000 \times |e_2(t)|)dt, \tag{5}$$

where t_f is set to be a sufficiently long time, so the integral value beyond this time can be neglected.

The performance of the designed R-PID controller was compared and verified against the IMC method [32], the Sadeghi method [33], the LopezITAE method [34], and the Skogestad method [35]. The controller parameters for the IMC, Sadeghi, LopezITAE, and Skogestad methods were determined by obtaining the steady-state gain K , the time constant T , and the time delay L from the FOPTD (First-Order Plus Time Delay) model. The FOPTD model of the gas turbine engine was approximated using the RCGA from the third-order system in (3). Figure 3 illustrates the RCGA adaptation for approximation with the FOPTD model. The parameters of the FOPTD model to be explored with the RCGA were searched using the objective function given in (6) to find the three parameters K , T , and L .

$$J_0 = \int_0^{t_f} |y_p - y_m|dt, \tag{6}$$

where y_p and y_m are the outputs of the third-order gas turbine engine model and the FOPTD model, respectively. t_f is the sufficiently large final integration time such that the integral values beyond this time can be neglected.

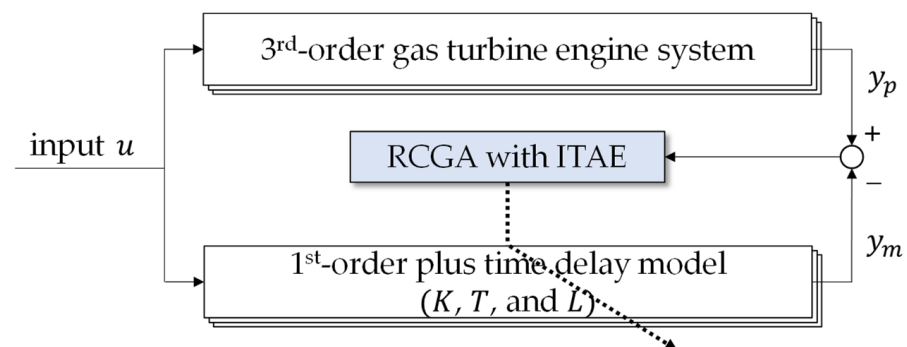


Figure 3. The RCGA adaptation for approximation with the FOPTD model.

5. Simulation of Gas Turbine Engine with RCGA-Based PID Speed Controller

5.1. Exploration of FOPTD Model Parameters for G_{Pi} Using RCGA

The FOPTD model is as follows.

$$G_M(s) = \frac{Y(s)}{U(s)} = \frac{K_M e^{-L_M s}}{1 + T_M s}, \tag{7}$$

A unit step input is applied for a certain period to both the third-order model $G_P(s)$ in (3) and the FOPTD model $G_M(s)$ in (7). The parameters are explored using the RCGA to minimize the objective function J_0 in (6). The population size for the RCGA is set to $N = 40$ with genetic operators using a reproduction coefficient $\eta = 2.0$, crossover probability $P_c = 0.95$, and mutation probability $P_m = 0.1$. Table 3 shows the parameters of the FOPTD model explored for each operating point [21].

Table 3. Parameters of G/T engine FOPTD model using RCGA.

Model	$G_{M1}(s)$	$G_{M2}(s)$	$G_{M3}(s)$
Operating point	6500 [r/min]	7500 [r/min]	8500 [r/min]
Gain (K_M)	1446.603	1028.121	608.734
Time constant (T_M)	4.47	2.878	1.494
Time delay (L_M)	0.724	0.418	0.316

5.2. RCGA-Based PID Controller

The control parameters of the RCGA used to explore the R-PID controller parameters for each operating point of the gas turbine engine model are population size $N = 50$, reproduction coefficient $\eta = 1.5$, crossover probability $P_c = 0.98$, and mutation probability $P_m = 0.1$. Table 4 presents the parameters of each explored controller along with M_s (maximum sensitivity).

Table 4. Controller parameters for each operating point of gas turbine engine.

Model	Tuning Method	Parameters for PID Controller				M_s
		K_P	T_I	T_D	K_a	
$G_{P1}(s)$	Proposed (R-PID1)	0.0030	5.3480	0.1870	2.6230	1.6030
	IMC ($T_c = 0.741$)	0.0030	4.8320	0.3349	2	1.7579
	Sadeghi	0.0044	6.5565	0.3506	2	2.8466
	LopezITAE	0.0031	3.4521	0.2521	2	1.6825
	Skogestad	0.0021	4.4700	0	2	1.5486
$G_{P2}(s)$	Proposed (R-PID2)	0.0040	3.2530	0.0961	2.7705	1.6360
	IMC ($T_c = 0.553$)	0.0039	3.0870	0.1949	2	1.6819
	Sadeghi	0.0069	4.2003	0.2033	2	3.5680
	LopezITAE	0.0048	2.2297	0.1467	2	1.9178
	Skogestad	0.0033	2.8780	0	2	1.7198
$G_{P3}(s)$	Proposed (R-PID3)	0.0040	1.5340	0.0440	2.2750	1.5430
	IMC ($T_c = 0.393$)	0.0049	1.6520	0.1429	2	1.6517
	Sadeghi	0.0082	2.2238	0.1512	2	2.8611
	LopezITAE	0.0059	1.1429	0.1080	2	1.8745
	Skogestad	0.0039	1.4940	0	2	1.6819

The M_s , used to verify the relative stability or robustness against uncertainty, can be obtained from the sensitivity function $S(j\omega)$ of the controller $C(j\omega)$ and the plant $P(j\omega)$.

The magnitude of this sensitivity function in the frequency domain can be expressed as follows.

$$|S(j\omega)| = \frac{1}{1 + C(j\omega)P(j\omega)}, \tag{8}$$

The maximum sensitivity M_s , representing the maximum magnitude of this sensitivity function at a specific frequency, can be expressed as follows.

$$M_s = \max_{0 \leq \omega \leq \infty} |S(j\omega)| = \max_{0 \leq \omega \leq \infty} \left| \frac{1}{1 + C(j\omega)P(j\omega)} \right| = \|S_\infty\|, \tag{9}$$

The magnitude of M_s is the inverse of the shortest distance to the critical point $(-1, j0)$ on the Nyquist plot of the open-loop transfer function. Therefore, a smaller value indicates that the Nyquist path passes farther from the critical point, allowing for more robust control [36,37].

5.3. Performance of R-PID Controllers at Each Operating Point

Simulations to verify the performance of the R-PID controller were conducted by distinguishing between nominal and uncertain plants. The nominal plant refers to the G_P in (3). The uncertain plant is set by increasing the gain and time delay of the nominal plant G_P by 5% each while simultaneously decreasing the time constant by 5%. To quantitatively compare the simulation results, the controllers were evaluated in terms of transient response, error, and control input.

Metrics such as rising time T_r , settling time T_s , and percentage overshoot (%OS) were used for evaluating transient response characteristics [38,39]. An error evaluation index, as shown in (10), was employed to consider the impact of the error on the control system.

$$ITAE = \int_0^{t_f} t \times |e(t)| dt, \tag{10}$$

Here, t_f is the final time of the simulation.

In (11), TV represents the total variation in the control input and is used as a measure of the smoothness of the control input [35]. A smaller TV indicates fewer aggressive changes in the control input, which is considered indicative of a superior controller.

$$TV = \sum_{k=1}^{n_s} |u_{k+1} - u_k|, \tag{11}$$

Here, u_k is the discretized value of the control input $u(t)$, and n_s is the number of discretized samples.

5.3.1. Application of R-PID1 to the G_{P1} Model

1. Nominal plant

The tracking performance of the R-PID1 controller was verified for the nominal plant G_{P1} at the operating point of 6500 [r/min]. Figure 4 shows each controller's tracking performance and fuel flow rate when the system, initially at 5500 [r/min], receives a step reference input of 6500 [r/min] at $t = 1$ s. Table 5 summarizes the performance metrics for a quantitative comparison of each controller, comparing the proposed controller (R-PID1) with the other controllers (IMC, Sadeghi, LopezITAE and Skogestad).

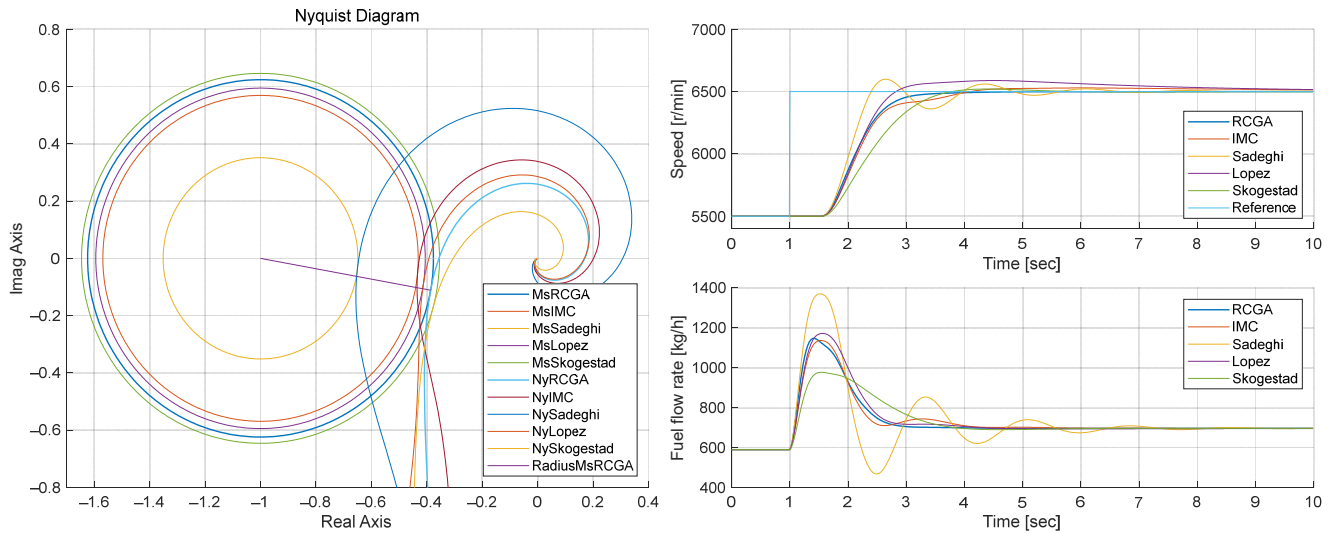


Figure 4. Sensitivity functions and step responses for nominal plant G_{P1} with controllers.

Table 5. Tracking performance for nominal plant G_{P1} .

Tuning Method	Tracking Performance					
	T_r	T_s (1%)	%OS	ITAE	TV	M_s
Proposed (RCGA)	0.9830	2.8928	0	866.9870	5.9098	1.6030
IMC ($T_c = 0.741$)	1.1206	10.5875	2.9106	1855.500	6.3842	1.7579
Sadeghi	0.5643	5.4502	9.9122	1173.500	15.5605	2.8466
LopezITAE	0.8159	10.3151	8.8324	2572.700	6.5833	1.6825
Skogestad	1.3714	4.1860	2.0215	1340.300	4.2384	1.5486

The transient response performance was examined from the perspective of a 1000 [r/min] change in reference input and the need for the gas turbine to stabilize at the reference operating point as quickly as possible. The rise time of the R-PID1 controller is slower than that of the Sadeghi method. Still, it has no overshoot and reaches the reference operating point most stably and quickly (1% T_s , 2.8928). The IMC method exhibits overshoot (%OS, 2.9106) and the slowest settling time (1% T_s , 10.5875) among the controllers, operating approximately 7.6947 s slower than the proposed controller. The Sadeghi method shows the fastest rise time but a relatively high overshoot (%OS, 9.9122). Its settling time (1% T_s , 5.4502) is about 2.5574 s slower than that of the proposed controller.

The ITAE error evaluation index is the smallest for the proposed controller at 866.9870, indicating superior performance.

The TV control input evaluation index is the second smallest for the proposed controller at 5.9098 after the Skogestad method, demonstrating that the control input of the proposed controller is stable without abrupt physical changes compared to the other controllers.

The robustness evaluation index M_s is the second smallest for the plant with the proposed controller applied at 1.6030 after the Skogestad method. This indicates that it passes farthest after the Skogestad method from the critical point $(-1, j0)$ in the Nyquist plot in Figure 4, showing that the controller is robust. The Sadeghi method has the largest M_s at 2.8466, indicating the lowest stability.

The TV and M_s of the Skogestad method is smaller than that of the proposed controller. Still, it has no overshoot and reaches the reference operating point most stably (ITAE, 866.9870) and quickly (1% T_s , 2.8928). The tracking performance of the proposed controller is better than that of the Skogestad method, which is the smallest TV and M_s . Therefore, it can be concluded that the controller proposed and explored using the RCGA exhibits

overall superior performance compared to other controllers. This performance can be assessed as highly suitable from the perspective of gas turbine applications in naval vessels requiring rapid maneuverability.

1. Uncertain plant

Under the condition that the FMU parameters remain unchanged, it is considered that the gas generator gain and time delay of the gas turbine engine change by +5% and −5% for the time constant, respectively. This accounts for variations in steady gain as the gas turbine engine operates in various harsh marine environments, as well as modeling errors and parameter uncertainties.

Table 6 presents the quantitative comparison of performance metric values of R-PID1 with other controllers and also shows the maximum sensitivity function M_s as a robustness evaluation index.

Table 6. Tracking performance for ±5 [%] change in uncertain plant G_{P1} .

Tuning Method	Tracking Performance					
	T_r	T_s (1%)	%OS	ITAE	TV	M_s
Proposed (RCGA)	0.7790	3.4884	3.3359	896.4249	6.3185	1.7450
IMC ($T_c = 0.741$)	0.7966	9.6632	3.2166	1604.000	7.0818	1.9364
Sadeghi	0.5060	9.0056	22.2146	1977.800	20.7071	3.6485
LopezITAE	0.6968	9.8433	12.6944	2391.400	7.0999	1.8472
Skogestad	1.1454	6.2637	5.8878	1529.600	4.4982	1.6603

Compared to the performance of the nominal plant (Table 5), it is observed that M_s generally increases as parameters change, indicating a decrease in stability. Still, the proposed controller shows a minor change in M_s (+0.142). The Sadeghi method exhibits the largest change in M_s (+0.8019). As shown in Figure 5, the Nyquist plot of the R-PID1 controller passes farthest from the critical point $(-1, j0)$ after the Skogestad method.

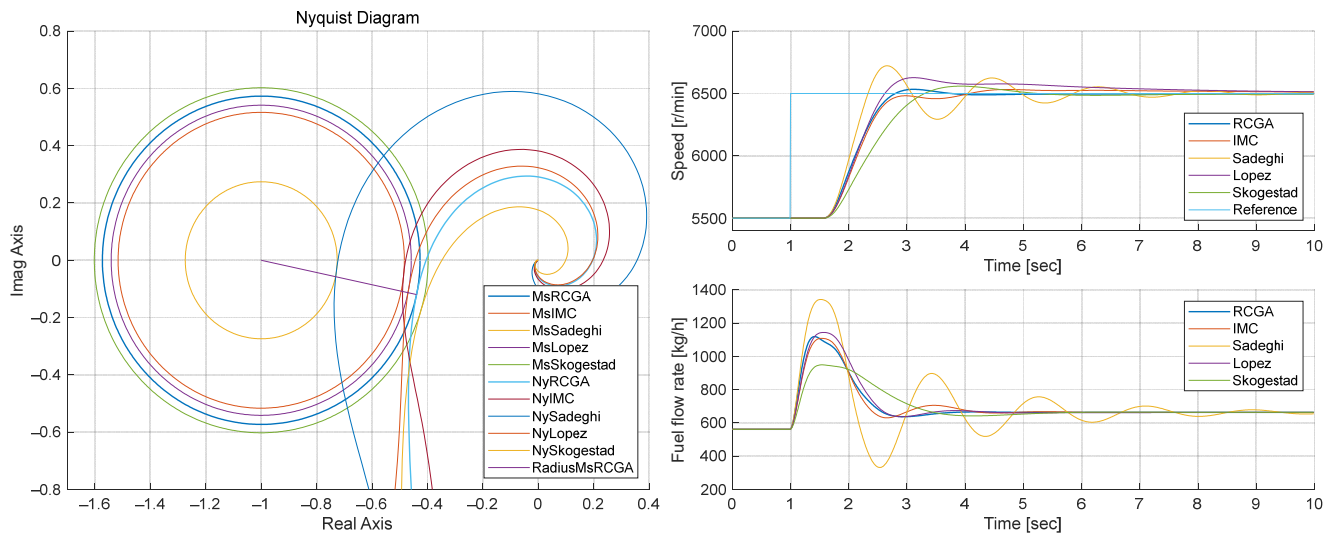


Figure 5. Sensitivity functions and step responses for uncertain plant G_{P1} with controllers.

When comparing the transient response results of the controllers for the uncertain plant (Table 6) with those for the nominal plant (Table 5), the rise times are shorter, and the overshoots are larger for the uncertain plant. The proposed controller has the shortest settling time, while the IMC method has the smallest overshoot.

The TV and M_s of the Skogestad method is smaller than that of the proposed controller. Still, it reaches the reference operating point most stably (ITAE, 896.4249) and quickly

(1% T_s , 3.4884). The tracking performance of the proposed controller is better than that of the Skogestad method. Therefore, it is evident that the proposed controller remains superior even when considering uncertainties.

5.3.2. Application of R-PID2 to the G_{P2} Model

1. Nominal plant

The tracking performance of the R-PID2 controller was verified for the nominal plant G_{P2} at the operating point of 7500 [r/min]. Figure 6 shows each controller’s tracking performance, fuel flow rate, and control input when the system, initially at 6500 [r/min], receives a step reference input of 7500 [r/min] at $t = 1$ s. Table 7 summarizes the performance metrics for a quantitative comparison of each controller, comparing the proposed controller (R-PID2) with the other controllers (IMC, Sadeghi, LopezITAE, and Skogestad).

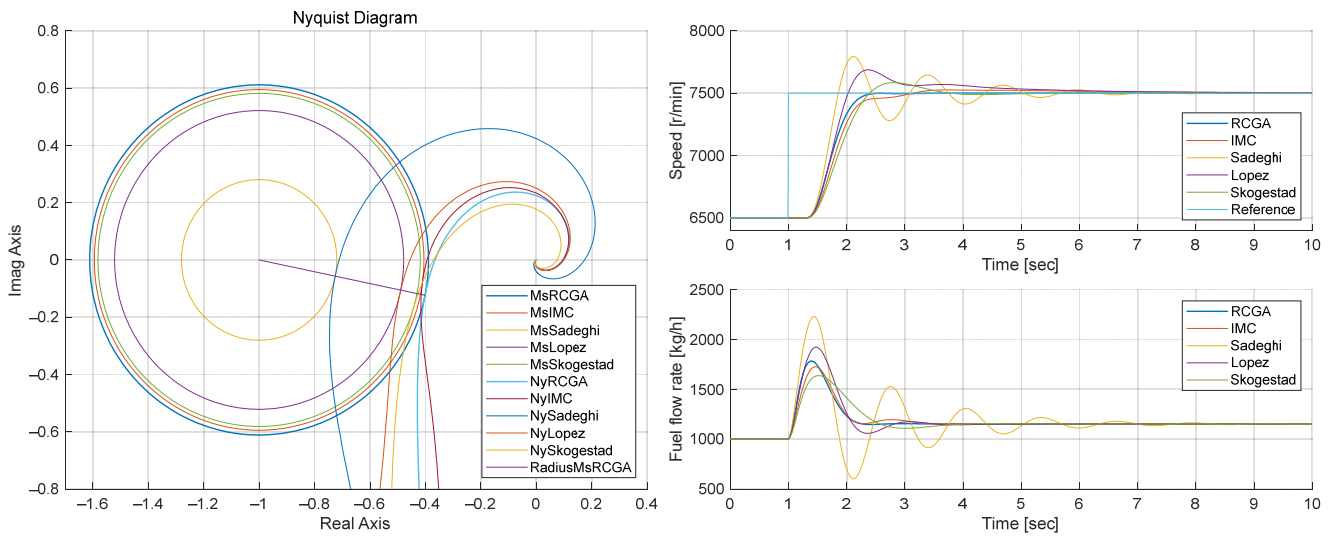


Figure 6. Sensitivity functions and step responses for nominal plant G_{P2} with controllers.

Table 7. Tracking performance for nominal plant G_{P2} .

Tuning Method	Tracking Performance					M_s
	T_r	T_s (1%)	%OS	ITAE	TV	
Proposed (RCGA)	0.6035	1.3715	0	336.2807	7.8657	1.6360
IMC ($T_c = 0.553$)	0.6758	6.3459	2.5431	886.4994	8.0206	1.6819
Sadeghi	0.3468	6.4032	29.3467	1093.500	32.6521	3.5680
LopezITAE	0.4585	6.2858	18.6795	1130.300	11.4022	1.9178
Skogestad	0.6996	3.5586	8.4345	623.7719	7.1666	1.7198

The transient response performance was examined from the perspective of a 1000 [r/min] change in reference input and the need for the gas turbine to stabilize at the reference operating point as quickly as possible. The rise time of the R-PID2 controller is slower than that of the Sadeghi method. Still, it has no overshoot and reaches the reference operating point most stably and quickly (1% T_s , 1.3715). The IMC method exhibits overshoot (%OS, 2.5431) and a settling time (1% T_s , 6.3459) that is approximately 4.9744 s slower than that of the proposed controller. The Sadeghi method shows the fastest rise time but has a relatively high overshoot (%OS, 29.3467). Its settling time (1% T_s , 6.4032) is the slowest among the controllers, operating about 5.0317 s slower than the proposed controller.

The ITAE error evaluation index is the smallest for the proposed controller at 336.2807, indicating superior performance.

The TV control input evaluation index is also the second smallest for the proposed controller at 7.8657 after that of the Skogestad method at 7.1666, demonstrating that the control input of the proposed controller is stable without abrupt physical changes compared to the other controllers.

The robustness evaluation index for the plant with the proposed controller applied is the smallest M_s at 1.6360. The Nyquist plot in Figure 6 indicates that it passes farthest from the critical point $(-1, j0)$, showing that the controller is robust. The Sadeghi method has the largest M_s at 3.5680, indicating the lowest stability. Therefore, it can be concluded that the controller proposed and explored using the RCGA exhibits overall superior performance compared to other controllers.

2. Uncertain plant

Under the condition that the FMU parameters remain unchanged, it is considered that the gas generator gain and time delay of the gas turbine engine change by +5% and the time constant by -5%, respectively. This accounts for variations in steady gain as the gas turbine engine operates in various harsh marine environments, as well as modeling errors and parameter uncertainties.

Table 8 presents the quantitative comparison of performance metric values of R-PID2 with the other controllers and also shows the maximum sensitivity function M_s as a robustness evaluation index. Compared to the performance of the nominal plant (Table 7), it is observed that M_s generally increases as parameters change, indicating a decrease in stability. Still, the proposed controller shows the most minor change in M_s (+0.1457). The Sadeghi method exhibits the most significant change in M_s (+1.6340). As shown in Figure 7, the Nyquist plot of the R-PID2 controller passes farthest from the critical point $(-1, j0)$.

Table 8. Tracking performance for ± 5 [%] change in uncertain plant G_{P2} .

Tuning Method	Tracking Performance					
	T_r	T_s (1%)	%OS	ITAE	TV	M_s
Proposed (RCGA)	0.5014	2.5034	6.6437	431.5650	8.5991	1.7817
IMC ($T_c = 0.553$)	0.5513	5.6160	2.9042	744.9939	8.8316	1.8377
Sadeghi	0.3193	9.9707	43.2646	2815.300	51.7848	5.2020
LopezITAE	0.4132	6.0048	28.7605	1062.400	13.1836	2.1682
Skogestad	0.6100	3.8675	15.2283	803.8700	7.8722	1.8774

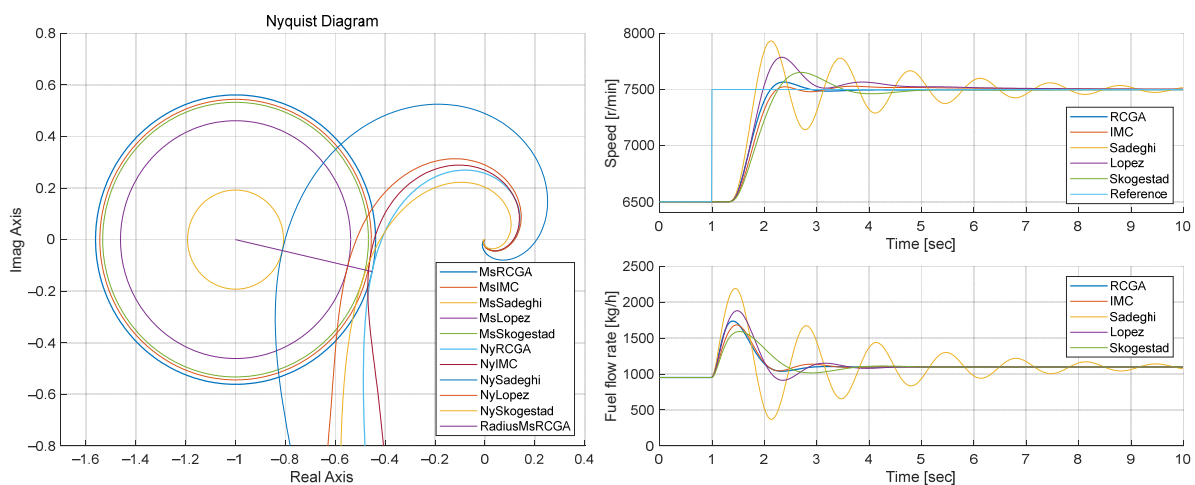


Figure 7. Sensitivity functions and step responses for uncertain plant G_{P2} with controllers.

When comparing the transient response results of the controllers for the uncertain plant (Table 8) with those for the nominal plant (Table 7), the rise times are shorter, and the

overshoots are more prominent for the uncertain plant. The proposed controller has the shortest settling time, while the IMC method has the smallest overshoot.

The ITAE is the smallest for the proposed controller, and the TV (8.5991) is the second smallest after that of the Skogestad method at 7.8722, indicating superior performance in control input changes. Therefore, it is evident that the proposed controller remains superior even when considering uncertainties.

5.3.3. Application of R-PID3 to the G_{P3} Model

1. Nominal plant

The tracking performance of the R-PID3 controller was verified for the nominal plant G_{P3} at the operating point of 8500 [r/min]. Figure 8 shows each controller’s tracking performance, fuel flow rate, and control input when the system, initially at 7500 [r/min], receives a step reference input of 8500 [r/min] at $t = 1$ s. Table 9 summarizes the performance metrics for a quantitative comparison of each controller, illustrating the proposed controller (R-PID3) against the other controllers (IMC, Sadeghi, LopezITAE, and Skogestad).

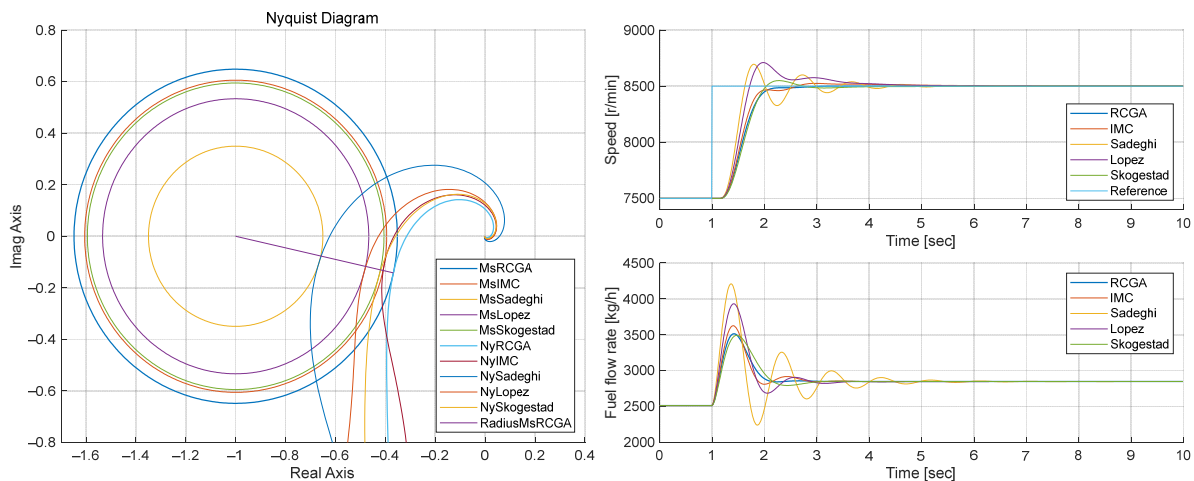


Figure 8. Sensitivity functions and step responses for nominal plant G_{P3} with controllers.

Table 9. Tracking performance for nominal plant G_{P3} .

Tuning Method	Tracking Performance					
	T_r	T_s (1%)	%OS	ITAE	TV	Ms
Proposed (RCGA)	0.5621	1.6937	0.0232	226.9119	7.4308	1.5430
IMC ($T_c = 0.393$)	0.4933	3.8149	2.4924	381.4974	9.9738	1.6517
Sadeghi	0.2916	3.7554	19.4849	410.3876	31.8313	2.8611
LopezITAE	0.3510	3.6521	21.0092	479.7164	13.9565	1.8745
Skogestad	0.5428	2.5661	4.9494	311.1299	7.8599	1.6819

The transient response performance was examined from the perspective of a 1000 [r/min] change in reference input and the need for the gas turbine to stabilize at the reference operating point as quickly as possible. The rise time of the R-PID3 controller is slower than that of the other controllers, but it has a slight overshoot (%OS, 0.0232). It reaches the reference operating point most quickly (1% T_s , 1.6937) and stably. The IMC method exhibits overshoot (%OS, 2.4924) and the slowest settling time (1% T_s , 3.8149) among the controllers, operating approximately 2.1212 s slower than the proposed controller. The Sadeghi method shows the fastest rise time but a relatively high overshoot (%OS, 19.4849). Its settling time (1% T_s , 3.7554) is about 2.0617 s slower than that of the proposed controller.

The ITAE error evaluation index is the smallest for the proposed controller at 226.9119, indicating superior performance. The TV control input evaluation index is also the smallest for the proposed controller at 7.4308, demonstrating that the control input of the proposed controller is stable without abrupt physical changes compared to the other controllers.

The robustness evaluation index M_s is the smallest for the plant with the proposed controller applied at 1.5430. The Nyquist plot in Figure 8 indicates that it passes farthest from the critical point $(-1, j0)$, showing that the controller is robust. The Sadeghi method has the largest M_s at 2.8611, indicating the lowest stability. Therefore, it can be concluded that the controller proposed and explored using the RCGA exhibits overall superior performance compared to other controllers.

1. Uncertain plant

Under the condition that the FMU parameters remain unchanged, it is considered that the gas generator gain and time delay of the gas turbine engine change by +5% and the time constant by -5%, respectively. This accounts for variations in steady gain as the gas turbine engine operates in various harsh marine environments, as well as modeling errors and parameter uncertainties.

Table 10 presents the quantitative comparison of performance metric values of R-PID3 with the other controllers and also shows the maximum sensitivity function M_s as a robustness evaluation index. Compared to the performance of the nominal plant (Table 9), it is observed that M_s generally increases as parameters change, indicating a decrease in stability. Still, the proposed controller shows the most minor change in M_s (+0.1021). The Sadeghi method exhibits the most considerable change in M_s (+0.8034). As shown in Figure 9, the Nyquist plot of the R-PID3 controller passes farthest from the critical point $(-1, j0)$.

Table 10. Tracking performance for ± 5 [%] change in uncertain plant G_{P3} .

Tuning Method	Tracking Performance					M_s
	T_r	T_s (1%)	%OS	ITAE	TV	
Proposed (RCGA)	0.4771	2.0158	2.9140	243.7229	7.9133	1.6451
IMC ($T_c = 0.393$)	0.4216	3.3301	2.9679	326.2124	10.9792	1.7914
Sadeghi	0.2675	5.6310	29.0833	806.8515	44.0989	3.6645
LopezITAE	0.3207	3.5403	28.6763	449.5882	15.8819	2.0874
Skogestad	0.4785	2.7077	10.4049	377.4220	8.5399	1.8142

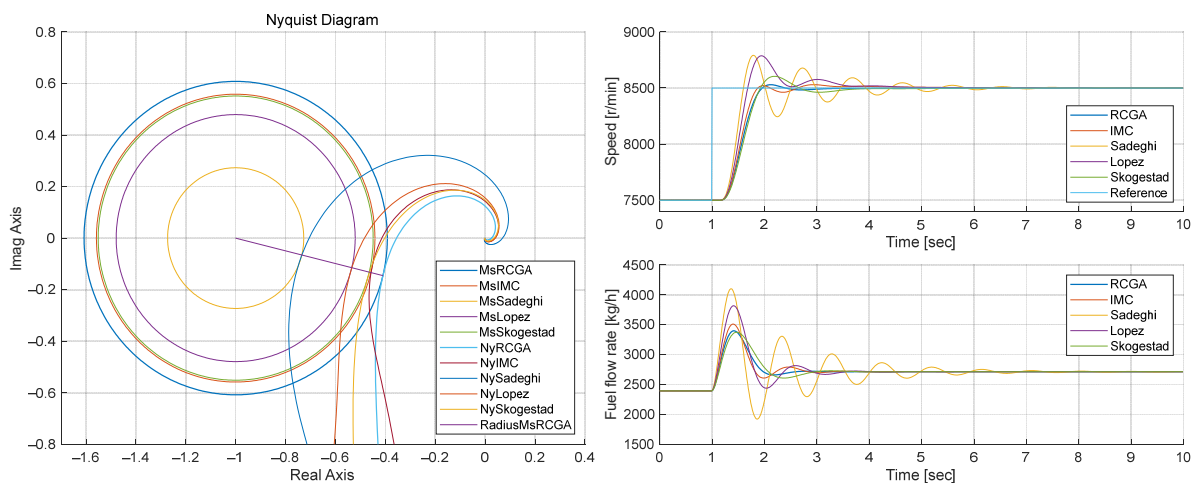


Figure 9. Sensitivity functions and step responses for uncertain plant G_{P3} with controllers.

When comparing the transient response results of the controllers for the uncertain plant (Table 10) with those for the nominal plant (Table 9), the rise times are shorter, and the overshoots are more significant for the uncertain plant. The proposed controller has the shortest settling time and the smallest overshoot.

The ITAE is the smallest for the proposed controller, and the TV (7.9133) is also the smallest, indicating superior performance in control input changes. Therefore, it is evident that the proposed controller remains superior even when considering uncertainties.

5.3.4. Application of R-PID $_i$ ($i = 1, 2, 3$) to the Entire Sub-Model G_{P_i} ($i = 1, 2, 3$)

Figure 10 applies each R-PID $_i$ ($i = 1, 2, 3$) controller to the entire sub-model G_{P_i} ($i = 1, 2, 3$). The transient response results are compared in Table 11.

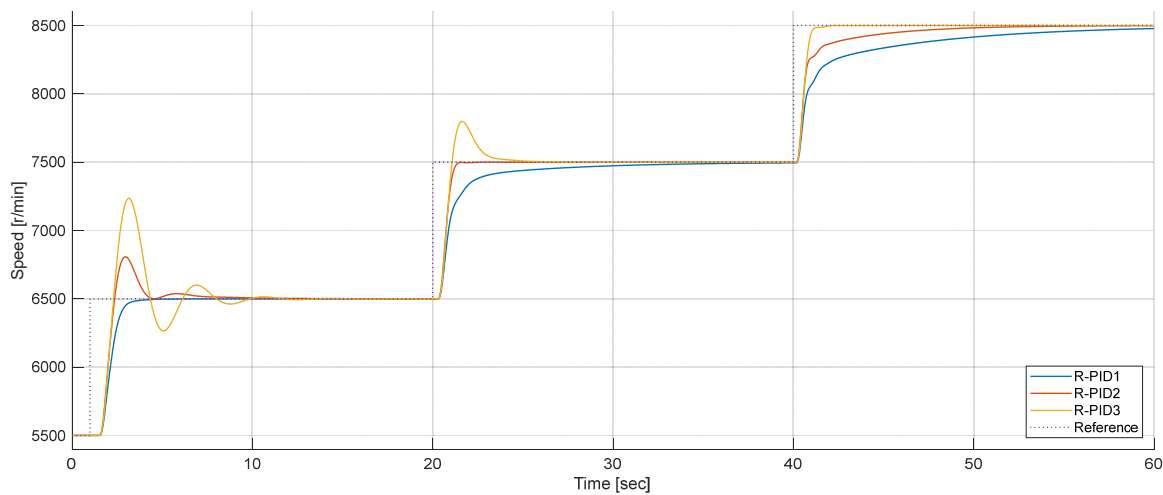


Figure 10. Step responses for applying R-PID $_i$ ($i = 1, 2, 3$) to G_{P_i} ($i = 1, 2, 3$).

Table 11. Performance comparison for each controller and sub-model.

Operation Point	T_r	R-PID1			R-PID2			R-PID3		
		T_s (1%)	%OS		T_r	T_s (1%)	%OS	T_r	T_s (1%)	%OS
6500 [rpm]	0.9839	2.8928	0	0.5633	8.0935	30.7304	0.5137	10.1441	75.5034	
7500 [rpm]	2.4070	15.9070	0	0.6035	1.3715	0	0.5003	4.8776	29.8651	
8500 [rpm]	8.3543	26.0139	0	2.6988	12.1901	0	0.5621	1.6937	0.0232	

Applying the R-PID1 controller across the entire rotational speed range of the sub-model G_{P_i} ($i = 1, 2, 3$) shows excellent performance at the 6500 [r/min] operating point, but rise and settling times increase at the 7500 [r/min] and 8500 [r/min] operating points. Particularly at the 8500 [r/min] operating point, the settling time (1% T_s , 26.0139) becomes extended.

Applying the R-PID2 controller across the entire rotational speed range of the sub-model G_{P_i} ($i = 1, 2, 3$) shows excellent tracking performance at the design operating point of 7500 [r/min]. However, at the 6500 [r/min] operating point, a significant control input causes an overshoot (%OS, 30.7304). At 8500 [r/min], the response is faster than with the R-PID1 controller but still has extended settling and rise times.

Applying the R-PID3 controller across the entire rotational speed range of the sub-model G_{P_i} ($i = 1, 2, 3$) shows superior tracking performance at the design operating point of 8500 [r/min]. However, the control input increases at the 6500 [r/min] operating point, increasing the fuel supply. This leads to significant overshoot (%OS, 75.5034) and severe hunting. There is also a considerable overshoot (%OS, 29.8651) at the 7500 [r/min] operating point.

The simulation results above show that the R-PID $_i$ ($i = 1, 2, 3$) controllers demonstrate satisfactory response performance at their tuned operating points. However, when operating outside the designed operating points, there can be delays in reaching a steady state or significant overshoot, leading to degraded response performance.

5.3.5. Application of R-PID $_i$ ($i = 1, 2, 3$) to Each Sub-Model G_{P_i} ($i = 1, 2, 3$) with Measurement Noise

In actual control environments, there is always the possibility of noise being introduced from sensors during signal measurement, which should be considered in controller design. To investigate the impact of noise on the proposed method, it is assumed that white Gaussian noise with normal distribution $N(0, 10)$ is introduced into the feedback sensor (rotational speed output). Figure 11 applies each R-PID $_i$ ($i = 1, 2, 3$) controller to each sub-model G_{P_i} ($i = 1, 2, 3$) with noise. Although the control input experiences fluctuations due to the noise, the rotational speed output demonstrates a response that, on average, does not cause significant distortion, remaining within approximately ± 10 rpm.

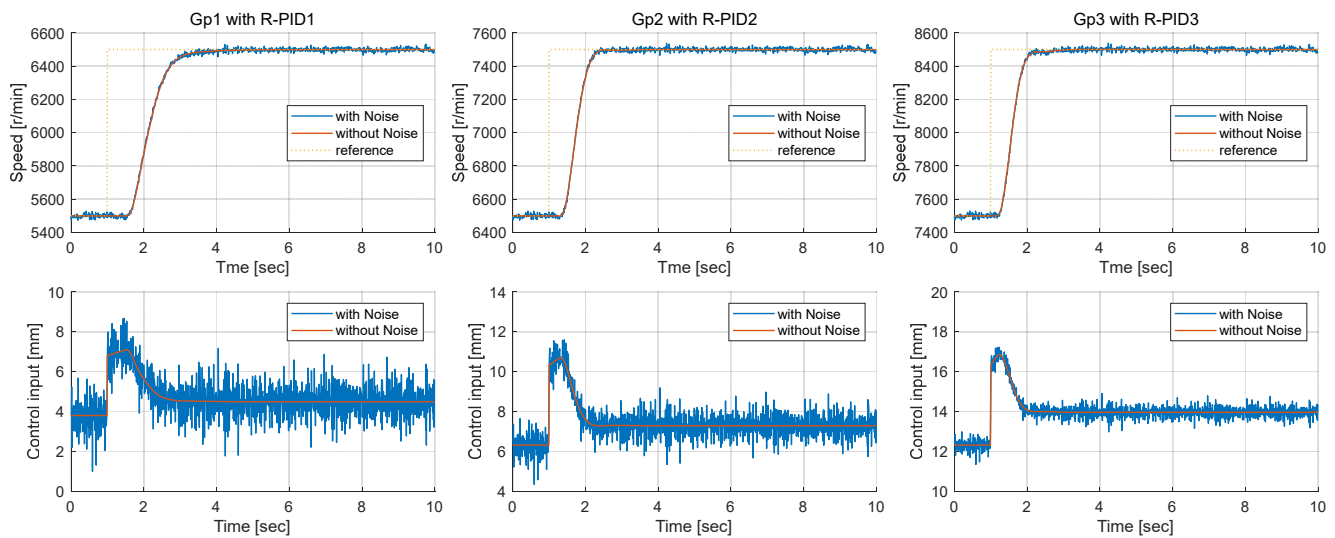


Figure 11. Step responses with noise for applying R-PID $_i$ ($i = 1, 2, 3$) to G_{P_i} ($i = 1, 2, 3$).

6. Discussion and Conclusions

Gas turbine engines used at sea are nonlinear systems with significant parameter variations due to frequent fluctuations and changes in the marine environment. This makes precise tracking control at a given specific rotational speed challenging. In this study, the propulsion type of the gas turbine engine is considered to be a system where four LM-2500 gas turbine engines operate simultaneously in a COGAG system. For mathematical modeling, a third-order model including time delay was derived at three operating points using actual commissioning data to reflect the inherent characteristics of the gas turbine engine. The cascade controller design involved designing an R-PID controller that explores the parameters of a PID controller using the RCGA for the models obtained at each operating point. In exploring two internal/external controller parameters simultaneously using the RCGA, an ITAE evaluation function was selected to rapidly minimize even small errors by assigning weights to elapsed time, thereby shortening the settling time among transient response characteristics. The ITAE evaluation function is more suitable for systems with uncertainties. If an appropriate evaluation function can be selected according to the system's characteristics, the RCGA can search for optimal controller parameters. Consequently, it was possible to find optimal controller parameters that satisfy the smallest ITAE evaluation function while being superior from an energy consumption perspective (TV),

having a short settling time (T_s , 1%), and a small percentage overshoot (%OS). Moreover, the maximum sensitivity (M_s), a relative stability measure, was between 1.3 and 2.0, as suggested in previous studies [36,37]. When quantitatively comparing various controllers, the maximum sensitivity (M_s) serves as a critical metric, particularly for evaluating robustness under uncertainty. Uncertainty refers to cases where gas turbine engines encounter harsh environments and modeling errors. Thus, while this study does not represent a real-world operational environment, it can partially reflect real-world conditions. The proposed R-PID controller satisfies $M_s < 2.0$, indicating that it exhibits greater robustness than other controllers, even under various harsh environments and modeling errors that may occur in real-world conditions. Through comparison with other controllers, it was evident that the R-PID controller exhibits superior relative stability across most operating ranges, indicating that it is a more stable system even among stable systems. In the application of R-PID1 to the G_{P1} model case, the TV and M_s of the Skogestad method were superior to those of R-PID1. However, the transient response characteristics of the dynamic system were not as favorable as those of R-PID1. This suggests that the R-PID1 possesses superior characteristics to the Skogestad method in reaching the desired speed smoothly yet as quickly as possible.

By applying the R-PID controller designed at each operating point to each model and conducting simulations, the following conclusions were drawn:

1. Comparing the M_s values obtained from the sensitivity function to verify robustness against uncertainties, it was confirmed that the R-PID controllers optimized with the RCGA for each operating point passed farthest from the critical point $(-1, j0)$ in the Nyquist path.
2. A comparison of M_s values for uncertain plants considering parameter variations was conducted to further investigate the robustness of the R-PID controller against uncertainties. The results showed that the R-PID controller had the smallest M_s value. Additionally, it was observed that the change in M_s value was also the least.
3. A quantitative comparison of the transient response characteristics of the R-PID controller with traditional control methods such as IMC, Sadeghi, LopezITAE, and Skogestad showed that while the rise time T_r was slightly slower, it demonstrated superior performance in terms of total variation in control input TV , settling time T_s (1%), overshoot %OS, and ITAE. It also showed excellent performance for uncertain plants with parameter variations.
4. The R-PID controller designed at a specific operating point exhibited excellent tracking control performance for the corresponding model. However, when moving beyond the designed operating point, it was observed that the rise time T_r and settling time T_s (1%) increased, and the overshoot %OS became larger, significantly deteriorating the tracking response performance. This indicates that the controllers designed for each operating point can maintain their performance only at that point and cannot guarantee performance beyond it.

The performance evaluation of the controller in this study is intended to design the controller and quantitatively compare it with other controllers within a computer simulation environment prior to their application in real-time applications. If applied to real-time applications, the evaluation of control performance should be newly conducted, taking into account the various internal environments (such as displacement, trim, hull resistance) and external environments (such as waves, currents, wind) of different ships, as well as the specific control requirements of the gas turbine engine operators.

In this study, however, the performance metrics used for controller evaluation (rise time T_r , settling time T_s , and overshoot %OS) reflect the critical RPM tracking capability required in actual naval vessels. This is well aligned with the requirements for rapid

maneuverability, which is a critical attribute of gas turbine engines utilized in operational naval vessels. Moreover, the maximum sensitivity M_s assesses the robustness of the controller against changes in marine environmental conditions. These evaluation criteria, although derived from a computer simulation environment, indirectly account for real-time operational conditions. This implies that the computational efficiency presented in this study can be largely justified for real-time marine applications.

This study acknowledges the limitation that the proposed controllers designed for specific operating points can maintain optimal performance only within those points. Nevertheless, it contributes to the field by developing a mathematical model of a gas turbine engine and proposing a control design methodology tailored to such operating conditions. This suggests that more advanced control methods must be applied for effective speed control of gas turbine engines with parameter variations and nonlinear characteristics. Therefore, the aim of future research will focus on integrating the mathematical models and R-PID controllers for three operating points into a fuzzy logic-based control system, ensuring consistent and robust performance across all operating conditions. Furthermore, although the real-time implementation of an actual gas turbine engine poses substantial challenges, it remains a pivotal goal for future research endeavors.

Author Contributions: Conceptualization, Y.L., K.R. and J.A.; methodology, Y.L., G.S. and J.A.; software, K.R., J.K. and J.A.; validation, Y.L., G.S. and J.A.; formal analysis, K.R., J.K. and J.A.; investigation, K.R., G.S. and J.A.; resources, Y.L., K.R. and J.A.; data curation, K.R. and G.S.; writing—original draft preparation, Y.L. and K.R.; writing—review and editing, Y.L., G.S. and J.A.; visualization, K.R., G.S. and J.K.; supervision, Y.L. and J.A.; project administration, J.A.; funding acquisition, J.A. All authors have read and agreed to the published version of the manuscript.

Funding: This work was supported by the Research Resurgence under the Glocal University 30 Project at Gyeongsang National University in 2024.

Data Availability Statement: The datasets used and/or analyzed during the current study are available from the corresponding author upon reasonable request.

Conflicts of Interest: The authors declare no conflicts of interest.

References

1. Woodyard, D. *Pounder's Marine Diesel Engines and Gas Turbines*, 8th ed.; Elsevier: London, UK, 2004.
2. Choi, Y. Prospect and Status of Power Plant Gas Turbine. *J. KSME* **1993**, *33*, 3–13.
3. Jo, J.-S. Gas Turbine Engine. *Plant J.* **2007**, *3*, 21–34.
4. El-Gohary, M.M. Design of hydrogen marine gas turbine. *Alex. Eng. J.* **2007**, *45*, 42–53.
5. Mrzljak, V.; Mrakovčić, T. Comparison of COGES and Diesel-Electric Ship Propulsion Systems. *J. Marit. Transp. Sci.* **2016**, 131–148. [[CrossRef](#)]
6. Brady, C.O.; Luck, D.L. The Increased Use of Gas Turbines as Commercial Maritime Engines. *ASME J. Eng. Gas Turbines Power* **1994**, *116*, 428–433. [[CrossRef](#)]
7. Kim, S.; Kim, H.; Park, S.; Yun, S.; Kim, J. Transient Modeling and Control of Turboshift Engine. In Proceedings of the Korean Society for Aeronautical and Space Sciences, Pyeongchang, Republic of Korea, 17–18 April 2008.
8. Back, K.; Ki, J.; Huh, H. Study on Performance Modeling of a MT30 Gas Turbine Engine for Marine Ship Applications. *KSPE J. Korean Soc. Propuls. Eng.* **2021**, *25*, 12–18. [[CrossRef](#)]
9. Back, K.; Huh, H.; Ki, J. Modeling and Simulation of a Gas Turbine Engine for Control of Mechanical Propulsion Systems. *KSPE J. Korean Soc. Propuls. Eng.* **2021**, *25*, 43–52. [[CrossRef](#)]
10. Lee, W. Modeling of gas turbine control system. *JIEIE J. Korean Inst. Illum. Electr. Install. Eng.* **2000**, *14*, 26–30.
11. Guda, S.R.; Wang, C.; Nehrir, M.H. Modeling of Microturbine Power Generation Systems. *Electr. Power Compon. Syst.* **2006**, *34*, 1027–1041. [[CrossRef](#)]
12. Hannett, L.N.; Jee, G.; Fardanesh, B. A governor/turbine model for a twin-shaft combustion turbine. *IEEE Trans. Power Syst.* **1995**, *10*, 133–139. [[CrossRef](#)]
13. Shin, S.U.; Jung, D.S.; Cho, S.H.; Kim, J.E.; Kang, H.Y. Study on characteristic of servo-valve for flow control. In Proceedings of the Korean Society of Propulsion Engineers, Busan, Republic of Korea, 27–29 November 2019.

14. Lee, D.-Y.; Choi, H.-Y.; Park, J.-S.; Koo, J.-Y. A Study on Stability Improvement of Fuel Metering Unit for Air Breathing Engine. *JKSAS J. Korean Soc. Aeronaut. Space Sci.* **2006**, *34*, 76–81.
15. Mohamed, O.; Wang, J.; Khalil, A.; Limhabraxh, M. Predictive control strategy of a gas turbine for improvement of combined cycle power plant dynamic performance and efficiency. *SpringerPlus* **2016**, *5*, 980. [[CrossRef](#)] [[PubMed](#)]
16. Lee, Y.H.; So, M.O. Speed Control of Marine Gas Turbine Engine using Nonlinear PID Controller. *JNPR J. Navig. Port Res.* **2015**, *39*, 457–463. [[CrossRef](#)]
17. Cha, Y. DSP System Design for Gas Turbine Engine Control and Realization of Engine Simulator. Ph.D. Thesis, Changwon National University, Changwon, Republic of Korea, 2006.
18. Lee, C.-H. Design of an IMC-Based PID Controller for Speed Control of Warships G/T Engines. Ph.D. Thesis, Korea Maritime and Ocean University, Busan, Republic of Korea, 2022.
19. Shon, Y.C.; Kim, S.W.; Jee, W.H. Design of Robust Feedback Controller for Turbo Jet Engine: Time Domain Approach. *J. Korean Soc. Propuls. Eng.* **1998**, *2*, 38–46.
20. Cha, Y.B.; Koo, B.M.; Song, D.H.; Choi, J.K. Development of an Engine Simulator for Optimal Control System Implementation of a Gas Turbine Engine. *JICCE J. Korea Inst. Inf. Commun. Eng.* **2007**, *11*, 75–82.
21. Ryu, K. GA-based Fuzzy-PID Controller for LM-2500 Gas Turbine Engine. Ph.D. Thesis, Korea Maritime and Ocean University, Busan, Republic of Korea, 2023.
22. Holland, J.H. *Adaptation in Natural and Artificial Systems: An Introductory Analysis with Applications to Biology, Control, and Artificial Intelligence*; University of Michigan Press: Ann Arbor, MI, USA, 1975.
23. Fogel, L.J. Extending communication and control through simulated evolution. In *Bioengineering—An Engineering View: Proceedings of the Symp. Engineering Significance of the Biological Sciences*; San Francisco Press: San Francisco, CA, USA, 1968.
24. Schwefel, H.P. *Numerical Optimization of Computer Models*; John Wiley: Chichester, UK, 1981.
25. Michalewicz, Z. *Genetic Algorithms+ Data Structures = Evolution Programs*, 3rd ed.; Springer: Berlin/Heidelberg, Germany; New York, NY, USA, 1996.
26. Gen, M.; Cheng, R. *Genetic Algorithms and Engineering Design*; JOHN WILEY & SONS, INC.: NY, USA, 1997.
27. Jin, G.-G.; Joo, S.-R. A study on a real-coded genetic algorithm. *J. Inst. Control Robot. Syst.* **2000**, *6*, 268–275.
28. Pham, D.T.; Jin, G. A hybrid genetic algorithm. In *Critical Technology: Proceedings of the Third World Congress on Expert Systems (Seoul, Korea)*; Cognizant Communication Corporation: Putnam Valley, NY, USA, 1996.
29. Matyas, J. Random optimization. *Autom. Remote Control* **1982**, *26*, 246–253.
30. Grefenstette, J.J. Optimization of control parameters for genetic algorithms. *IEEE Trans. Syst. Man Cybern.* **1986**, *16*, 122–128. [[CrossRef](#)]
31. De Jong, K.A. Analysis of the Behavior of a Class of Genetic Adaptation Systems. Ph.D. Dissertation, The University of Michigan, Ann Arbor, MI, USA, 1975.
32. Garcia, C.E.; Morari, M. Internal model control-1: A unifying review and some new results. *Ind. Eng. Chem. Process Des. Dev.* **1982**, *21*, 308–323. [[CrossRef](#)]
33. Sadeghi, J.; Tych, W. Deriving new robust adjustment parameters for PID controller using scale-down and scale-up techniques with a new optimization method. In Proceedings of the ICSE: 16th Conference of System Engineering, Coventry, UK, 9–11 September 2003.
34. Lopez, A.M.; Miller, J.A.; Smith, C.L.; Murrill, P. Tuning controller with error-integral criteria. *Inst. Tech.* **1967**, *14*, 57–62.
35. Skogestad, S. Simple analytic rules for model reduction and PID controller tuning. *J. Process Control* **2003**, *13*, 291–309. [[CrossRef](#)]
36. Anil, C.; Padma Sree, R. Tuning of PID controllers for integrating systems using direct synthesis method. *ISA Trans.* **2015**, *57*, 211–219. [[CrossRef](#)] [[PubMed](#)]
37. Åström, K.J.; Hägglund, T. *PID Controllers: Theory, Design, and Tuning*, 2nd ed.; Instrument Society of America: Durham, NC, USA, 1995.
38. So, G.-B.; Yea, J.-H.; Zhao, H.-Y.; So, M.-O. Design of a PID Controller Based on Internal Model Control Technique for First Order Time Delay Processes. *J. Korean Soc. Fish. Mar. Sci. Educ.* **2022**, *34*, 1–9. [[CrossRef](#)]
39. Ahn, J.-K.; So, G.-B.; Lee, J.-Y.; Lee, Y.-H.; So, M.-O.; Jin, G.-G. PID Control of a Shell and Tube Heat Exchanger System Incorporating Feedforward Control and Anti-windup Techniques. *J. Inst. Control Robot. Syst.* **2014**, *20*, 543–550. [[CrossRef](#)]

Disclaimer/Publisher’s Note: The statements, opinions and data contained in all publications are solely those of the individual author(s) and contributor(s) and not of MDPI and/or the editor(s). MDPI and/or the editor(s) disclaim responsibility for any injury to people or property resulting from any ideas, methods, instructions or products referred to in the content.